Synthesis, characterization and crystal structure of *bis*[4-methyl-1-{1-(pyridin-2-yl)ethylidene}thiosemicarbazide-κ^3*S*,*N*,*N*]zinc(II)

ABSTRACT

Schiff base ligand (4-methyl-1-(1-(pyridin-2-yl)ethylidene)thiosemicarbazide (H_2L) was synthesized via condensation of 2-acetylpyridine and 4-methyl-3-thiosemicarbazide in ethanol. The Zn(II) complex was obtained from 2:1 (H_2L/$Zn(OAc)_2{\cdot}2H_2O$) molar ratio reaction, yielding a neutral compound formulated as $[Zn(HL)_2]$. Elemental analysis, ^{1}H and ^{13}C NMR, conductance measurements and FT-IR spectroscopy were used for the characterization of the ligand and the complex. The complex is non-electrolyte in DMF solution. The structure of the complex was determined by single crystal X-ray diffraction study. Two ligand coordinated the Zn(II) ion. Each of the azomethine ligand was coordinated to Zn(II) ion through one azomethine nitrogen atom, one pyridine nitrogen atom and one sulfur atom, yielding an octahedral Zn(II) complex. The compound crystallizes in the triclinic space group P-1 with unit cell dimensions a = 8.551 (6) Å, b = 10.948 (5) Å, c = 12.060 (4) Å, α = 91.66 (3)°, β = 100.03 (5)°, γ = 109.92 (3)°, V = 1040.5 (10) Å^3, Z = 2, R_1 = 0.066 and wR_2 = 0.158. The Zn(II) cation in N_4S_2 inner is situated in a distorted octahedral environment.

Keywords: FTIR, Zinc, acetylpyridine, ^{4}N-methylthiosemicarbazone, Octahedral, X-ray diffraction

1. INTRODUCTION

"Semicarbazone and thiosemicarbazone Schiff bases have been widely studied due to their diverse potentialities. Thiosemicarbazones are known to have a wide range of biological applications. They are used as anticancer" [1,2], antibacterial [3,4], antifungal [5,6], and biocides [7]. "Coordination complexes obtained from these Schiff bases are able to enhance or inhibit some of these properties" [8–11]. "In addition to the important biological properties observed, physical properties are noted. The original structures of these transition metal complexes formed with these Schiff bases lead to physical properties such as magnetism" [12,13], fluorescence [14,15] or catalysis [16,17]. "Thiosemicarbazone complexes are used in the synthesis of nanomaterials which are used in the photodegradation of dye molecules to depollute the contaminated environment" [18-20]. "Thiosemicarbazone Schiff bases are versatile and can coordinate in several ways. Detailed studies of the molecular structures and coordination mode of these Schiff bases are carried out. In the thiosemicarbazide moiety, a thione/thiol equilibrium can be established such that the sulfur atom can bind to the metal in its thione or thiolate form" [21,22] or remain free [23,24]. "When the thiosemicarbazone moiety is modified by the presence of a donor group on the nitrogen atom, as in the case of 4-methyl-3-thiosemicarbazide, deprotonation can be facilitated, thus allowing the sulfur atom to react in its thiolate form" [25,26]. In our previous work we have reported the preparation and the X-ray structures of Co(II/III), Ni(II) and Zn(II) complexes derived from 1-(1-hydroxypropan-2-ylidene)thiosemicarbazide [27]. In this paper, we report the synthesis and structural characterization of the Schiff base (4-methyl-1-(1-(pyridin-2-yl)ethylidene)thiosemicarbazide (H_2L)) and the X-ray diffraction structure of its complex with Zn(II).

2. MATERIAL AND METHODS

2.1. Starting materials and Instrumentations

2-acetylpyridine, 4-methyl-3-thiosemicarbazide, and zinc acetate dihydrate were commercial products (from Aldrich) and were used without further purifications. The solvents were reagent grade and were purified by usual methods. Elemental analyses were carried out using a VxRio EL Instrument. The FTIR spectra were recorded on a FTIR Spectrum Two of Perkin Elmer (4000–400 cm$^-$

[1]). The ^{1}H and ^{13}C NMR spectra of the Schiff base were recorded in DMSO-d_6 on a BRUKER 500 MHz spectrometer at room temperature using TMS as an internal reference. The molar conductance of 10^{-3} M solution of the metal complex in DMF was measured at 25 °C using a WTW LF-330 conductivity meter with a WTW conductivity cell.

2.2. Synthesis of ligand (4-methyl-1-(1-(pyridin-2-yl)ethylidene)thiosemicarbazide (H_2L)

The ligand H_2L was synthetized using the procedure described by Hazani et al. [28] with slight modification. A solution of 2-acetylpyridine (1.2114 g, 0.010 mol) in 20 mL of methanol was slowly added to a solution of 4-methyl-3-thiosemicarbazide (1.1919 g, 0.010 mol) in 20 mL of methanol. Two drops of glacial acetic acid were added. The mixture was refluxed for 2 h. On cooling, the white product which was formed was filtered off and recrystallized in ethanol. Yield, 90 %. M.P. 176°C. Anal. Calc for $C_9H_{12}N_4S$: C, 51.90; H, 5.81; N, 26.90; S, 15.39. Found: C, 51.86; H, 5.76; N, 26.83; S, 15.33. IR (cm^{-1}): 3235 ($\nu_{N—H}$), 3170 ($\nu_{N—H}$), 1552 ($\nu_{C=N}$), 1259 and 818 ($\nu_{NH-C=S}$). ^{1}H NMR (DMSO-d_6, δ(ppm)): 2.70 (S, 3H, -N=C-CH_3); 3.12 (D, 3H, -NCH_3); 7.33-8.65 (m, 4H, =CH_{Py}); 8.96 (s, H, HN-Me) ; 12.05 (s, H, HN). ^{13}C NMR (DMSO-d_6, δ(ppm)): 13.25 (-N=C-CH_3); 32.15 (-N=C-CH_3); 121-150 (C_{Ar}); 156.32 (C=N); 180.01 (N-C=S).

2.3. Synthesis of the Zn(II) complex

In a round bottomed flask, H_2L (0.4182 g, 2 mmol) and 15 mL of ethanol were mixed. Under stirring, a solution of $Zn(OAC)_2{\cdot}2(H_2O)$ (0.2195 g ; 1 mmol) in 5 mL of ethanol was added and the resulting mixture was refluxed for two hours. After cooling, the yellow solution was filtered off and left for slow evaporation. Yellow crystals suitable for X-ray diffraction analysis were collected after two weeks. Yield: 60 %. Anal. Calc for $C_{18}H_{22}N_8S_2Zn$: C, 45.05; H, 4.62; N, 23.35; S, 13.36. Found: C, 45.02; H, 4.60; N, 23.31; S, 13.32. IR (cm-1): 3224 (νN—H), 1599 ($\nu_{C=N}$), 728 (ν_{C-S}). ^{1}H NMR (DMSO-d_6, δ(ppm)): 2.63 (S, 3H, -N=C-CH_3); 2.98 (D, 3H, -NCH_3); 7.03-8.15 (m, 4H, =CH_{Py}); 8.02 (s, H, HN-Me). ^{13}C NMR (DMSO-d_6, δ(ppm)): 12.31 (-N=C-CH_3); 35.33 (-NCH_3); 123-148 (C_{Ar}); 144.56 (-N=**C**-CH_3); 170.12 (S-**C**=N). Conductance Λ ($S{\cdot}cm^2{\cdot}mol^{-1}$): 14 (fresh solution) et 13.75 (two weeks after).

2.4. X-ray structure determination of complex 1

"The ethanol solution of Zn(II) complex was left to slow evaporation and yellow crystals suitable for X-ray analyze were formed after two weeks. The details of the X-ray crystal structure solution and refinement are given in Table 1. Measurements were made on a Bruker SMART CCD Area Detector. All data were corrected for Lorentz and polarization effects. Empirical absorption correction was applied. Complex scattering factors were taken from the program package *SHELXTL"* [29]. "The structure was solved by direct methods, which revealed the position of all non-hydrogen atoms. The structure was refined on F^2 by a full-matrix least-squares procedure using anisotropic displacement parameters for all non-hydrogen atoms" [30]. "All hydrogen atoms were located in their calculated positions and refined using a riding model. Molecular graphics were generated using *ORTEP-3"* [31].

Table 1. Crystallographic data and refinement parameter for the complex.

Empirical formula	$C_{18}H_{22}N_8S_2Zn$
M_r	479.92
Crystal system, space group	Triclinic, *P-1*
a (Å)	8.551 (6)
b (Å)	10.948 (5)
c (Å)	12.060 (4)
α (°)	91.66 (3)
β (°)	100.03 (5)

γ (°)	109.92 (3)
V (Å^3)	1040.5 (10)
Z	2
D_{calc} (gcm^{-3})	1.532
Mo $K\alpha$ (Å)	0.71073
T (K)	293
μ (mm^{-1})	1.40
F(000)	496
Crystal size (mm)	0.22 × 0.21 × 0.12
θ range (°)	3.3-30.0
No. of measured reflections	16394
No. of independent reflections	5910
No. of observed [$I > 2\sigma(I)$] reflections	3853
R_{int}	0.101
$R[F^2 > 2\sigma(F^2)]$	0.066
$wR(F^2)$	0.158
Goodness-of-fit on F^2	1.15
No. of reflections	5910
No. of parameters	262
$\Delta\rho_{max}$, $\Delta\rho_{min}$ (e Å^{-3})	0.65, −0.58

3. RESULTS AND DISCUSSION

3.1. General study

The infrared spectrum of the free ligand shows two bands at 3235 and 3170 cm^{-1} which are attributed to the NH stretching vibrations. The stretching vibrations bands due to the C=N and C=S groups appear, respectively, at 1552 and 1259 cm^{-1}. The vibrations of the pyridine ring are pointed between 1580 and 1450 cm^{-1}. "No band due to the SH stretching vibration appears in the infrared spectrum of the ligand between 2600 and 2500 cm^{-1}. This suggests that the ligand is in its thione form. The FT-IR spectrum of the studied complex shows a broad band at 3224 cm^{-1} attributed to the NH vibration of the thioamide. The medium intensity absorption band pointed at 1599 cm^{-1} is due to the stretching vibration (CH=N) of the imine group whose nitrogen atom is coordinated to the metal. This is in agreement with the vibrations found for complexes derived from thiosemicarbazone ligands" [31]. The strong bands due to the pyridine ring are observed between 1563–1525 cm^{-1}, while the characteristic band of the N-N vibration is found at 1025 cm^{-1}. The presence of a weak intensity band pointed at 728 cm^{-1}, attributed to the C-S stretching vibration and the absence of a band due to the C=S stretching vibration at around 1259 cm^{-1}, show that the ligand is coordinated in its thiolate form [31]. The ^{1}H NMR spectrum for the Zn(II) complex shows the absence of the proton of the hydrazino group NH which is pointed in the spectrum of the free ligand at 12.05 ppm. This confirms that the ligand coordinates to the zinc(II) ion in its monodeprotonated form. The signal assigned to the proton of the -NH-CH$_3$ motif is shifted towards high fields and appears on the spectrum of the complex at 8.02 ppm while it appears on the spectrum of the ligand at 8.96 ppm. This behavior is already reported for similar complexes [26]. "The

signals of the aromatic protons of the free ligand which are in the range 7.33-8.65 ppm are shifted in the spectrum of the complex in the range 7.03-8.15 ppm, indicating that the magnetic environment of the aromatic ring has changed. This shows, clearly, the involvement of the nitrogen atom in coordination with the zinc ion. In the ^{13}C NMR spectrum of the ligand, the signals of the carbon atoms of C=N and C=S appeared at 156.32 (-N=**C**-CH_3) and 180.01 (N-HN-**C**=S) ppm, respectively. After coordination, the displacement of the two signals that appear at 144.56 ppm and 170.12 ppm is observed. They are attributed, respectively, to -N=**C**-CH_3 and N-N=**C**-S. We note the transformation of N-HN-C=S to N-N=C-S-. These facts confirm, on the one hand, the deprotonation of the ligand, and on the other hand, the involvement of the nitrogen atom of the azomethine function and the sulfur atom in its thiolate form in the coordination of the zinc ion" [25]. The Zn(II) complex exhibits molar conductivity of 14 $\Omega^{-1}\cdot cm^2\cdot mol^{-1}$ which indicate that the complex is neutral in nature [32]. This value remains almost constant over time, indicating the good stability of the complex in DMF solution.

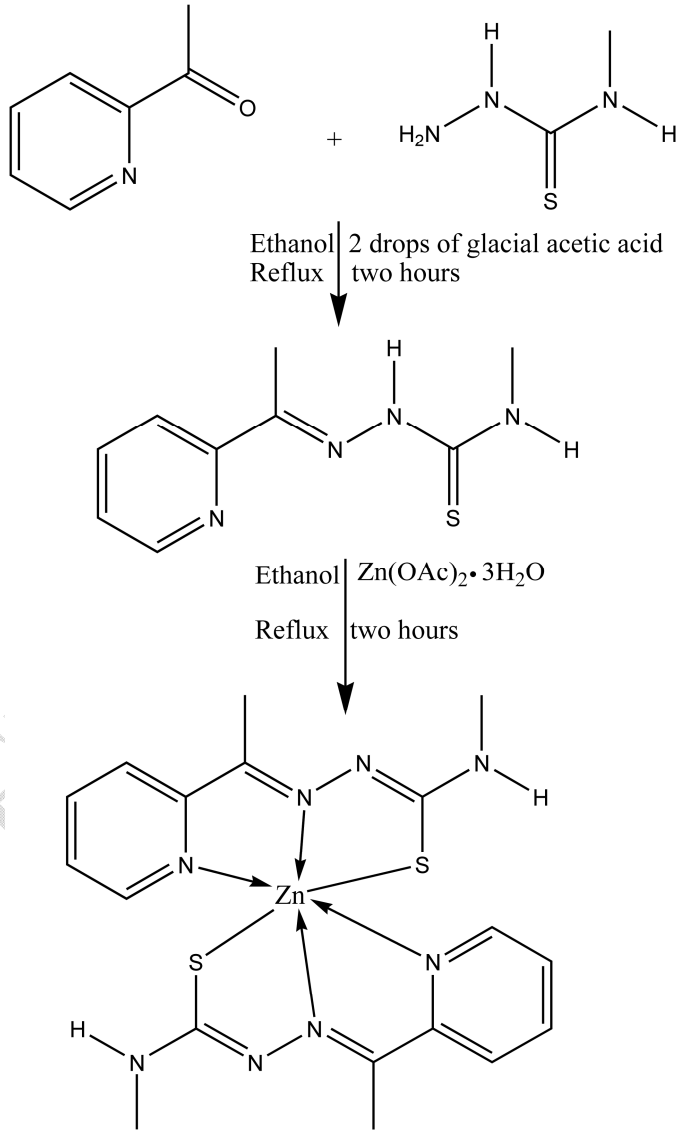

Scheme 1. Syntheses of the ligand H_2L and its Zn(II) complex preparation.

3.2. Description of the structure

The X-ray analysis shows that the compound crystallizes in a triclinic system with a space group P-1. Selected bonds distances and angles are reported in Table 2. The molecular structure of the compound

with the atomic labelling scheme is shown in Figure 1. The asymmetric unit contains two ligand molecules and one Zn(II) ion. The ligand molecules are monodeprotonated. Each of the two ligand molecules is coordinated to the zinc ion through one nitrogen atom of azomethine function, one nitrogen atom of the pyridine ring and one sulfur atom in thiolate form. Thus the complex is neutral, and the metal center is hexacoordinated. The zinc atom is located in an octahedral environment. The basal plane of the coordination polyhedron is composed of a sulfur atom (S2), two nitrogen atoms of the two imino functions (N2 and N6) and a pyridine nitrogen atom (N5). The mean plane through the four atoms S2/N2/N6/N5 is essentially planar with a maximum deviation of 0.068 Å for S2. The Zinc(II) atom is located at 0.158 Å from the mean plane defined by the atoms occupying the base of the octahedron. The *cissoid* angles are in the range [73.23(14)°-111.65(11)°] while the *transoid* angles are 152.93(10)° [S2-Zn-N5] and 163.38(15)° [N2-Zn-N6]. The sum of the angles subtended by the atoms in the basal plane is 358.97°. The apical positions are occupied by the nitrogen atom N1 of a pyridine ring and the sulfur atom S1 forming an angle S1-Zn1-N1 of 153.19(10)°. The values of these angles demonstrate that the environment around Zn(II) is strongly distorted. Each ligand forms two five-membered rings of ZnSCNN and ZnNCCN types. The bite angles are 79.49(10)° [S1-Zn1-N2] and 79.80(11)° [S2-Zn1-N6] for the first type of ring and 73.74(13)° [N1-Zn1-N2] and 73.23(14)° [N5-Zn1-N6] for the second type of ring. The ligands are quasi-planar with a maximum deviation of 0.114 Å for the C3 atom of the ligand containing S1 and a maximum deviation of 0.098 Å for the C17 atom of the ligand containing S2. The two mean planes of the ligands form a dihedral angle of 88.99°. The Zn-N_{Py} bonds [Zn1-N1 = 2.228(4) Å and Zn1-N5 = 2.219(4) Å] are longer than the Zn-N_{imino} bonds [Zn1-N2 = 2.127(3) Å and Zn1-N6 = 2.2.131(3) Å]. This shows that the azomethine nitrogen atoms are more strongly coordinated to Zn(II) than the nitrogen atoms of the pyridine rings. The Zn-S bond lengths [Zn1-S1 = 2.4368(17) Å and Zn1-S2 = 2.445(2) Å] are shorter than the Zn-S [2.600(1) Å and 2.535(1) Å] bond distances reported for similar complex [Zn(H_2dap-^{4}NMetsc(H_2O)$_2$](NO_3)$_2$·H_2O (H_2dap-^{4}NMetsc is 2,6-diacetylpyridine bis(^{4}*N*-methylthiosemicarbazone) in which the sulfur atom acts in its thione form [33]. They are also longer than the Zn-S [2.33583(8) Å and 2.3749(9) Å] distances in the complex [Zn(phthalsme)(DMF)] (phthalsme is phthalaldehyde bis(S-methyldithiocarbazonate)) in which the sulfur atom acts in its thiolate form [34]. Although the ligand acts in its monodeprotonated form, the C-S bond lengths [C8-S1 = 1.699(5) Å and C16-S2 = 1.698(4) Å] are intermediate between single C-S [1.56 Å] and double C-S [1.81 Å] bonds. In addition to this, it is noted that the adjacent C-N bond lengths are strengthened [C8-N3 = 1.288(6) Å and C16-N7 = 1.318(6) Å] and are shorter than double bond C-N [1.34-1.38 Å] bonds [35]. These facts are indicative of a delocalization of electrons on the Zn-S-C-N moieties [26]. No intramolecular hydrogen bond is present in the zinc complex. Intermolecular hydrogen bond of type C-H···S (C12—H12···S1^{i} : i = −*x*, −*y*, −*z*+1 and C7—H7A···S2^{ii} : ii = −*x*+1, −*y*+1) and C-H···N (C17—H17A···N8^{iii} : iii = −*x*+2, −*y*+1, −*z*+1) link the molecules into three-dimensional network architecture (Figure 2, Table 3). Figure 3 shows the crystal packing of the complex.

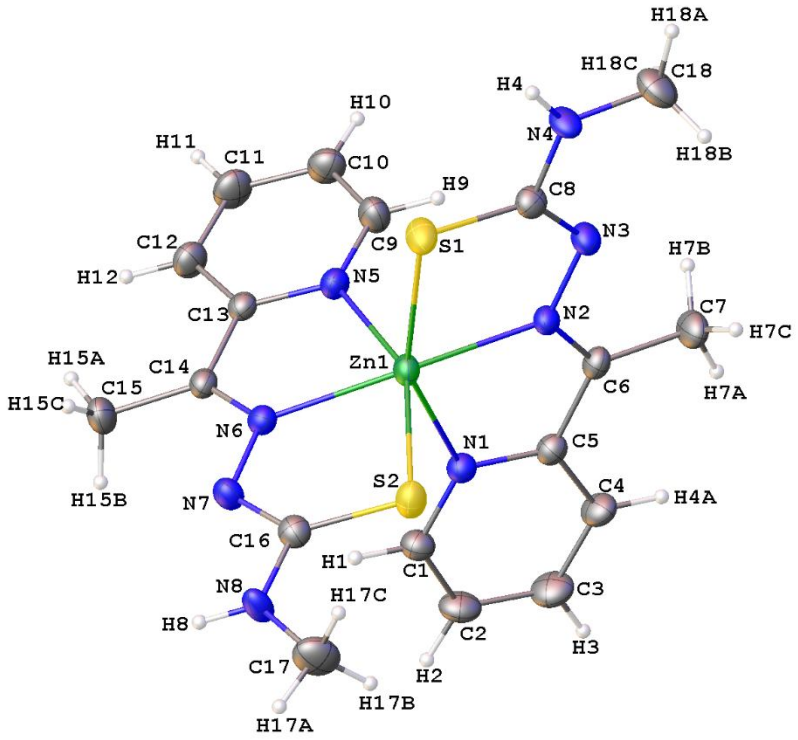

Figure 1:*ORTEP* plot (30% probability ellipsoids) showing the structure of the Zn(II) complex.

Table 2. Selected geometric parameters (Å, °).

Zn1—N2	2.127 (3)	Zn1—S2	2.445 (2)
Zn1—N6	2.131 (3)	S2—C16	1.698 (4)
Zn1—N5	2.219 (4)	S1—C8	1.699 (5)
Zn1—N1	2.228 (4)	N7—C16	1.318 (6)
Zn1—S1	2.4368 (17)	N3—C8	1.288 (6)
N2—Zn1—N6	163.38 (13)	N5—Zn1—S1	94.42 (11)
N2—Zn1—N5	94.29 (14)	N1—Zn1—S1	153.19 (10)
N6—Zn1—N5	73.23 (14)	N2—Zn1—S2	111.65 (11)
N2—Zn1—N1	73.74 (13)	N6—Zn1—S2	79.80 (11)
N6—Zn1—N1	94.70 (13)	N5—Zn1—S2	152.93 (10)
N5—Zn1—N1	89.03 (14)	N1—Zn1—S2	90.91 (11)
N2—Zn1—S1	79.49 (10)	S1—Zn1—S2	97.69 (6)
N6—Zn1—S1	111.77 (10)		

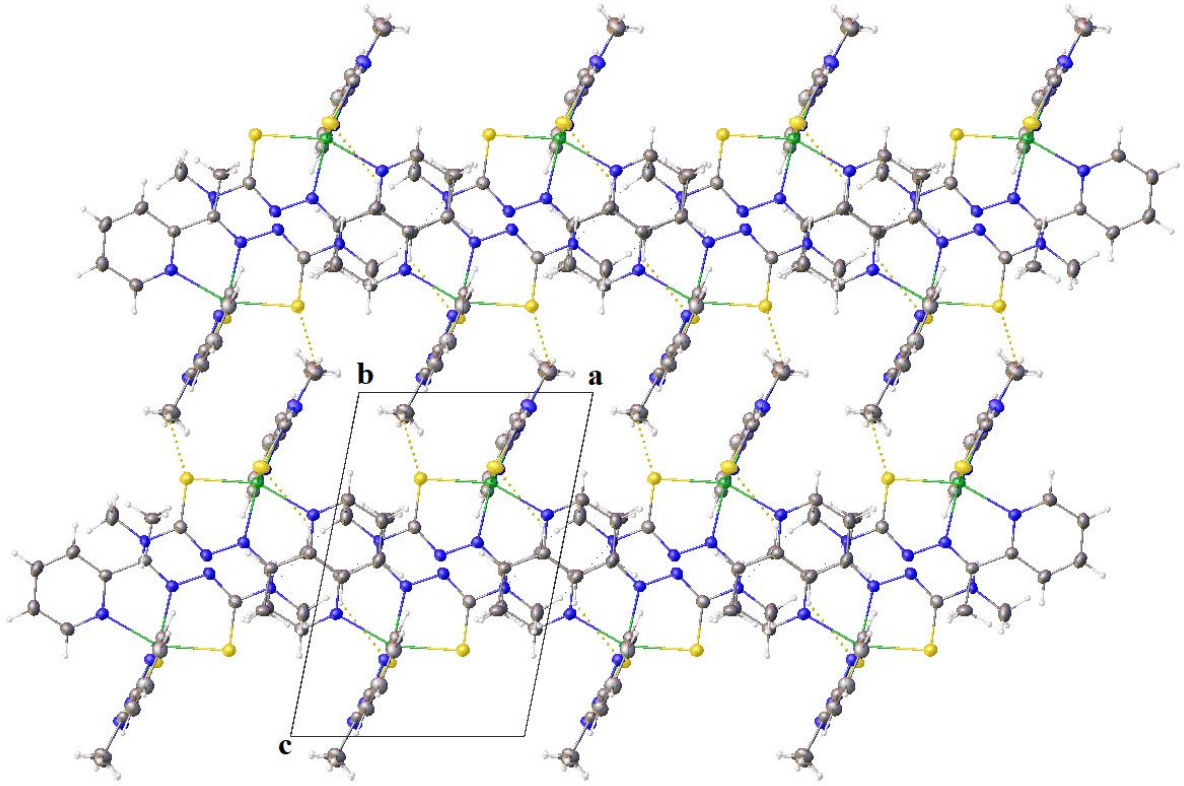

Figure 2: Layers of the complex parallel to the *b* axis.

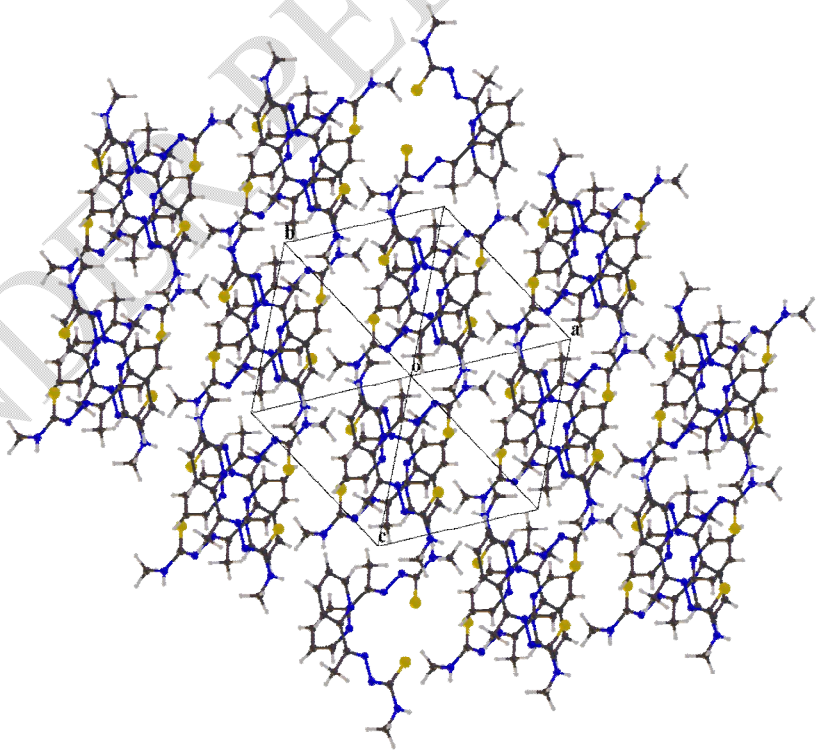

Figure 3: Crystal packing of the title compound.

Table 3. Hydrogen-bond geometry (Å, °).

D—H···*A*	D—H	H···*A*	D···*A*	D—H···*A*
C12—H12···S1^{i}	0.93	2.86	3.478(5)	124.7
C7—H7A···S2^{ii}	0.96	3.01	3.808(6)	141.6
C17—H17A···N8^{iii}	0.96	2.68	3.619(7)	165.3

Symmetry codes: (i) −*x*, −*y*, −*z*+1; (ii) −*x*+1, −*y*+1, −*z*+2; (iii) −*x*+2, −*y*+1, −*z*+1.

4. CONCLUSION

The reported work is concerned with the synthesis and the structural study of a mononuclear-complex derived from the organic molecular ligand, (4-methyl-1-(1-(pyridin-2-yl)ethylidene)thiosemicarbazide. The compounds are characterized by FTIR and ^{1}H and ^{13}C NMR spectroscopies. Additionally, the structure of the complex is studied by conductivity measurement and X-ray diffraction. The complex is a neutral electrolyte in DMF solution. Two monodeprotonated ligand molecules acting in tridentate fashion through one azomethine nitrogen atom, one pyridine nitrogen atom and one sulfur atom, yield a mononuclear neutral complex in which the Zn(II) is hexacoordinated. The environment around the zinc(II) ion is best described as a distorted octahedral polyhedron. Intramolecular hydrogen -bonds link the molecules into three-dimensional network.

5. SUPPORTING INFORMATION

CCDC-1844643 contains the supplementary crystallographic data for this paper. These data can be obtained free of charge via https://www.ccdc.cam.ac.uk/structures/, or by contacting The Cambridge Crystallographic Data Centre, 12 Union Road, Cambridge CB2 1EZ, UK.

Disclaimer (Artificial intelligence)

Option 1:

Author(s) hereby declare that NO generative AI technologies such as Large Language Models (ChatGPT, COPILOT, etc.) and text-to-image generators have been used during the writing or editing of this manuscript.

Option 2:

Author(s) hereby declare that generative AI technologies such as Large Language Models, etc. have been used during the writing or editing of manuscripts. This explanation will include the name, version, model, and source of the generative AI technology and as well as all input prompts provided to the generative AI technology

Details of the AI usage are given below:

1.

2.

3.

REFERENCES

1. Anisree, S., Shanmugavelan, P., Vijayalakshmi, P., Kishore, R., & Srivastava, N. (2024). (2024). Synthesis, characterization and anticancer screening of novel phenylbenzylidene thiosemicarbazone derivatives. Phosphorus, Sulfur, and Silicon and the Related Elements, 199(4), 267–276. https://doi.org/10.1080/10426507.2024.2330935
2. Chaudhary, U., Kumar, P., Sharma, P., Chikara, A., Barua, A., Mahiya, K., Subin, J. A., Yadav, P. N., & Pokharel, Y. R. (2024). Synthesis of 5-hydroxyisatin thiosemicarbazones, spectroscopic investigation, protein-ligand docking, and in vitro anticancer activity. Bioorganic Chemistry, 153, 107872. https://doi.org/10.1016/j.bioorg.2024.107872
3. Sharma, N., Dhingra, N., & Singh, H. L. (2024). Design, spectral, antibacterial and in-silico studies of new thiosemicarbazones and semicarbazones derived from symmetrical chalcones. Journal of Molecular Structure, 1307, 138000. https://doi.org/10.1016/j.molstruc.2024.138000
4. Swaminathan, J., Anbusrinivasan, P., & Vijayalakshmi, A. (2023). Synthesis, geometrical, spectral and antibacterial studies of 4-hydroxy-3-methoxybenzaldehyde thiosemicarbazone by experimental and theoretical investigations. Computational and Theoretical Chemistry, 1229, 114338. https://doi.org/10.1016/j.comptc.2023.114338
5. Gutsanu, V., & Lisa, G. (2020). Composites containing metal and thiosemicarbazone: Thermal, antimicrobial and antifungal properties. Polyhedron, 191, 114800. https://doi.org/10.1016/j.poly.2020.114800
6. Bajaj, K., Buchanan, R. M., & Grapperhaus, C. A. (2021). Antifungal activity of thiosemicarbazones, bis(thiosemicarbazones), and their metal complexes. Journal of Inorganic Biochemistry, 225, 111620. https://doi.org/10.1016/j.jinorgbio.2021.111620
7. Sousa, R. P. C. L., Teixeira, F., Costa, S. P. G., Figueira, R. B., & Raposo, M. M. M. (2024). Quinoline-based hydrazones for biocide detection: Machine learning-aided design of new TBT chemosensors. Dyes and Pigments, 225, 112053. https://doi.org/10.1016/j.dyepig.2024.112053
8. Adhikari, H. S., Garai, A., Khanal, C., & Yadav, P. N. (2024). Synthesis and comprehensive characterization with anticancer activity assessment of salicylaldehyde and 2-acetylphenol based chitosan thiosemicarbazones and their copper(II) complexes. Carbohydrate Polymer Technologies and Applications, 7, 100469. https://doi.org/10.1016/j.carpta.2024.100469
9. Misigo, W. O., Njenga, L. W., Odhiambo, R. A., Meyer, M., Julius, L., Sibuyi, N., Lalancette, R. E., & Onani, M. O. (2023). New thiosemicarbazones and their palladium(II) complexes: Synthesis, spectroscopic characterization, X-ray structure and anticancer evaluation. Inorganica Chimica Acta, 558, 121746. https://doi.org/10.1016/j.ica.2023.121746
10. Balakrishnan, N., Haribabu, J., Dharmasivam, M., Jayadharini, J. P., Anandakrishnan, D., Swaminathan, S., Bhuvanesh, N., Echeverria, C., & Karvembu, R. (2023). Influence of indole-*N* substitution of thiosemicarbazones in cationic Ru(II)(η^6-benzene) complexes on their anticancer activity. Organometallics, 42(3), 259–275. https://doi.org/10.1021/acs.organomet.2c00604
11. Nongpiur, C. G. L., Soh, C., Diengdoh, D. F., Verma, A. K., Gogoi, R., Banothu, V., Kaminsky, W., & Kollipara, M. R. (2023). 3-acetyl-coumarin-substituted thiosemicarbazones and their ruthenium, rhodium and iridium metal complexes: An investigation of the antibacterial, antioxidant and cytotoxicity activities. Journal of Organometallic Chemistry, 998, 122788. https://doi.org/10.1016/j.jorganchem.2023.122788
12. Rhoufal, F., Guesmi, S., Jouffret, L., Ketatni, E. M., Sergent, N., Hlil, E. K., Obbade, S., & Bentiss, F. (2022). Novel copper(II) and nickel(II) coordination complexes of 2,4-pentanedione bis-thiosemicarbazone: Synthesis, structural characterization, computational studies, and magnetic properties. Inorganic Chemistry Communications, 141, 109574. https://doi.org/10.1016/j.inoche.2022.109574
13. El-Ata, A. W. A., El-Gamil, M. M., El-Reash, Y. G. A., El-Reash, G. M. A., & Abozeid, S. M. (2024). Two New Inner-sphere Pt(II) Thiosemicarbazone Schiff base complexes immobilized into magnetic

nanoparticles: Synthesis, Characterization, and Biological Investigations. Inorganic Chemistry Communications, 170, 113366. https://doi.org/10.1016/j.inoche.2024.113366

14. Ranjani, M., Kalaivani, P., Dallemer, F., Selvakumar, S., Kalpana, T., & Prabhakaran, R. (2022). Fluorescent Cu(II) complex as chemosensor for the detection of l-Aspartic acid with high selectivity and sensitivity. Inorganica Chimica Acta, 530, 120683. https://doi.org/10.1016/j.ica.2021.120683
15. Lobana, T. S., Khanna, S., & Butcher, R. J. (2008). Synthesis of a fluorescent gold(I) complex with a thiosemicarbazone, $[Au_2(3\text{-}NO_2\text{-}Hbtsc)_4]Cl_2{\cdot}2CH_3CN$. Inorganic Chemistry Communications, 11(12), 1433–1435. https://doi.org/10.1016/j.inoche.2008.09.023
16. Priyarega, S., Haribabu, J., & Karvembu, R. (2022). Development of thiosemicarbazone-based transition metal complexes as homogeneous catalysts for various organic transformations. Inorganica Chimica Acta, 532, 120742. https://doi.org/10.1016/j.ica.2021.120742
17. Kaviani, N., Behrouz, S., Jafari, A. A., & Rad, M. N. S. (2024). Copper-hydroxyacetophenone thiosemicarbazone complex on silica-coated magnetite nanoparticles as an efficient catalyst for three-component synthesis of 1,4-disubstituted 1,2,3-triazoles. Journal of Organometallic Chemistry, 1007, 123043. https://doi.org/10.1016/j.jorganchem.2024.123043
18. Disale, S. D., & Garje, S. S. (2010, March). Growth of Nanocrystalline FeS and FeS2 Using Iron (II) Cinnamaldehyde Thiosemicarbazone Complexes as Single-Source Precursors. Text, American Scientific Publishers. https://doi.org/10.1166/asl.2010.1092
19. Suroshe, J. S., Mlowe, S., Garje, S. S., & Revaprasadu, N. (2018). Preparation of Iron Sulfide Nanomaterials from Iron(II) Thiosemicarbazone Complexes and Their Application in Photodegradation of Methylene Blue. *Journal of Inorganic and Organometallic Polymers and Materials*, *28*(3), 603–611. https://doi.org/10.1007/s10904-018-0816-9
20. Yepseu, A. P., Ngoudjou, L. E. T., Tigwere, G. A., Nyamen, L. D., Revaprasadu, N., Masikane, S., Boulet P., Cleymand F. & Ndifon, P. T. (2024). Hot injection synthesis of CuS decorated CdS and ZnS nanomaterials from metal thiosemicarbazone complexes as single source precursors: Application in the photocatalytic degradation of methylene blue. *Inorganic Chemistry Communications*, *166*, 112650. https://doi.org/10.1016/j.inoche.2024.112650
21. El-Gammal, O. A., Fouda, A. E.-A. S., & Nabih, D. M. (2020). Novel Mn^{2+}, Fe^{3+}, Co^{2+}, Ni^{2+} and Cu^{2+} complexes of potential OS donor thiosemicarbazide: Design, structural elucidation, anticorrosion potential study and antibacterial activity. Journal of Molecular Structure, 1204, 127495. https://doi.org/10.1016/j.molstruc.2019.127495
22. Refat, M. S., & El-Metwaly, N. M. (2012). Spectral, thermal and biological studies of Mn(II) and Cu(II) complexes with two thiosemicarbazide derivatives. Spectrochimica Acta Part A: Molecular and Biomolecular Spectroscopy, 92, 336–346. https://doi.org/10.1016/j.saa.2012.02.041
23. Başaran, E., Sıcak, Y., Sogukomerogullari, H. G., Karaküçük-Iyidoğan, A., Oruç-Emre, E. E., Sönmez, M., & Öztürk, M. (2019). Synthesis of novel chiral metal complexes derived from chiral thiosemicarbazide ligands as potential antioxidant agents. Chirality, 31(6), 434–444. https://doi.org/10.1002/chir.23069
24. Singh, A., Bharty, M. K., Dani, R. K., Singh, S., Kushawaha, S. K., & Singh, N. K. (2014). Manganese(II) and zinc(II) complexes of 4-phenyl(2-methoxybenzoyl)-3-thiosemicarbazide: Synthesis, spectral, structural characterization, thermal behavior and DFT study. Polyhedron, 73, 98–109. https://doi.org/10.1016/j.poly.2014.02.029
25. Hazani, N. N., Dzulkifli, N. N., Ghazali, S. A. I. S. M., & Mohd, Y. (2022). Synthesis, Characterisation and Corrosion Inhibition of Mild Steel by Butyltin(IV) 2-Acetylpyridine 4-Methyl-3-Thiosemicarbazone in HCl. Trends in Sciences, 19(12), 4615. https://doi.org/10.48048/tis.2022.4615

26. Pedrido, R., Bermejo, M. R., Romero, M. J., Vázquez, M., González-Noya, A. M., Maneiro, M., Rodríguez, M. J., & Fernández, M. I. (2005). Syntheses and X-ray characterization of metal complexes with the pentadentate thiosemicarbazone ligand bis(4-*N*-methylthiosemicarbazone)-2,6-diacetylpyridine. The first pentacoordinate lead(II) complex with a pentagonal geometry. Dalton Trans., (3), 572–579. https://doi.org/10.1039/B416296J
27. Ndoye, C., Excoffier, G., Seck, G. A., Diouf, O., Thiam, I. E., Sidibe, M., & Gaye, M. (2022). Crystal structures of bis[1-(1-hydroxypropan-2-ylidene)thiosemicarbazide-κ^3*S*,*N*,*O*)cobalt(III)-tetra(thiocyanato-κ*N*) cobalt(II) methanol solvate, bis{1-(1-hydroxypropan-2-ylidene)thiosemicarbazide-κ^3*S*,*N*,*O*}nickel(II) bis(thiocyanate) and (1-(1-hydroxypropan-2-ylidene)thiosemicarbazide-κ^3*S*,*N*,*O*)bis(thiocyanato-κ*N*)zinc(II). European Journal of Chemistry, 13(2), 196–205. https://doi.org/10.5155/eurjchem.13.2.196-205.2253
28. Hazani, N. N., Mohd, Y., Ghazali, S. A. I. S. M., & Dzulkifli, N. N. (2019). Electrochemical studies of thiosemicarbazone derivative and its tin(IV) complex as corrosion inhibitor for mild steel in 1 M hydrochloric acid. Chemistry Journal of Moldova. General, Industrial and Ecological Chemistry, 14(1), 98-106. http://dx.doi.org/10.19261/cjm.2019.545
29. Sheldrick, G. M. (2015). SHELXT – Integrated space-group and crystal-structure determination. Acta Crystallographica Section A, 71(1), 3–8. https://doi.org/10.1107/S2053273314026370
30. Sheldrick, G. M. (2015). Crystal structure refinement with SHELXL. Acta Crystallographica Section C, 71(1), 3–8. https://doi.org/10.1107/S2053229614024218
31. Farrugia, L. J. (2012). WinGX and ORTEP for Windows: an update. Journal of Applied Crystallography, 45(4), 849–854. https://doi.org/10.1107/S0021889812029111
32. Geary, W. J. (1971). The use of conductivity measurements in organic solvents for the characterisation of coordination compounds. Coordination Chemistry Reviews, 7(1), 81–122. https://doi.org/10.1016/S0010-8545(00)80009-0
33. Ali, M. A., Mirza, A. H., Chartres, J. D., & Bernhardt, P. V. (2011). Synthesis, characterization and X-ray crystal structures of seven-coordinate pentagonal-bipyramidal zinc(II), cadmium(II) and tin(IV) complexes of a pentadentate N_3S_2 thiosemicarbazone. Polyhedron, 30(2), 299–306. https://doi.org/10.1016/j.poly.2010.10.027
34. Ali, M. A., Mirza, A. H., Mei, C. C., Bernhardt, P. V., & Karim, M. R. (2013). Template synthesis and X-ray structural characterization of nickel(II) and zinc(II) complexes of tetradentate SNNS ligands formed by condensation of phthalaldehyde with S-methyldithiocarbazate and 4N-methyl-3-thiosemicarbazide. Polyhedron, 49(1), 277–283. https://doi.org/10.1016/j.poly.2012.10.008
35. Allen, F. H., Kennard, O., Watson, D. G., Brammer, L., Orpen, A. G., & Taylor, R. (1987). Tables of bond lengths determined by X-ray and neutron diffraction. Part 1. Bond lengths in organic compounds. J. Chem. Soc., Perkin Trans. 2, (12), S1–S19. https://doi.org/10.1039/P298700000S1